INFORMATION
Volume 19, Number 1, pp.17-23
ISSN 1343-4500

Positional Variance of the Hand based on Linear Quadratic Regulator in Two-Link Upper-Arm Reaching Movements

Yoshiaki Taniai*[1], Tomohide Naniwa[1], Munadi[2]
1. Graduate School of Engineering, University of Fukui, Fukui 910-8507, Japan,
2. Department of Mechanical Engineering, Diponegoro University, Semarang 50275, Indonesia
**E-mail: taniai@rbt.his.u-fukui.ac.jp*

Abstract

In upper-arm reaching movements, positional variances of the optimal trajectories based on optimal feedback control have been reported to exhibit a peak around the middle of the movement duration in a one-link arm model and in a mass point model. However, the variance in a two-link arm model has not been examined. In this study, we show that the positional variance of the hand of a two-link arm based on a linear quadratic regulator exhibits a peak around the middle of the movement duration and this property agrees with that of the measured trajectories of humans.

Keywords : two-link upper-arm reaching movement, optimal feedback control, linear quadratic regulator, positional variance

1 Introduction

In upper-arm reaching movements of humans, the trajectories of the hand are slight curves and their speed profiles are bell-shaped curves [1]. Furthermore, the positional variances of the hand exhibit a peak around the middle of the movement duration in iterative one-link upper-arm reaching movements [2] and in iterative two-link upper-arm reaching movements [3][4].

Todorov and Li (2005) proposed the iterative linear quadratic Gaussian method (iLQG) as an optimal feedback control for upper-arm reaching movements [5]. The results show that the optimal trajectories of the hand are slight curves and that the optimal speed profiles are bell-shaped curves. Furthermore, the optimal trajectories based on optimal feedback control have been reported to exhibit a reduction of the positional variance around the middle of the movement duration in a mass point model [4] or an inertial point model [6]. However, the characteristic of the positional variance of the hand in a two-link arm model has not been examined. In this study, we examined the positional variance of the hand based on a linear quadratic regulator (LQR) in the two-link upper-arm reaching movements.

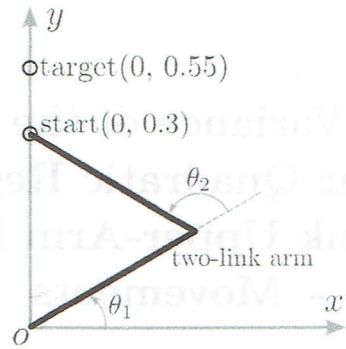

Figure 1: Task of a two-link upper-arm reaching movement in the horizontal plane.

2 Method

We obtained the optimal control signals by using an LQR for a nonlinear musculoskeletal system after its linearization and then computed the trajectories from the optimal control signals and signal-dependent noise. Finally, the positional variance of the hand was computed from the trajectories.

2.1 Task

Figure 1 shows the task of an upper-arm reaching movement. The start position $\boldsymbol{p}_s = (x_s, y_s)$ is (0, 0.3) [m], and the target position $\boldsymbol{p}_e = (x_e, y_e)$ is (0, 0.55) [m]. The movement duration is 0.35 s.

2.2 Musculoskeletal system

The musculoskeletal system is a two-link six-muscle arm model. The dynamics of the system $\boldsymbol{g}(\boldsymbol{x}, \boldsymbol{u})$ are as follows [7]:

$$\frac{d}{dt}\begin{bmatrix}\boldsymbol{q}\\ \dot{\boldsymbol{q}}\\ \boldsymbol{f}\end{bmatrix} = \boldsymbol{g}(\boldsymbol{x},\boldsymbol{u}) = \begin{bmatrix}\dot{\boldsymbol{q}}\\ \boldsymbol{M}^{-1}(\boldsymbol{q})(-\boldsymbol{C}(\boldsymbol{q},\dot{\boldsymbol{q}})+\boldsymbol{\tau})\\ \boldsymbol{T}^{-1}(-\boldsymbol{f}+\boldsymbol{f}_c(\boldsymbol{u}))\end{bmatrix} \tag{1}$$

where the state vector $\boldsymbol{x}$ denotes $[\boldsymbol{q}, \dot{\boldsymbol{q}}, \boldsymbol{f}]^T$, $\boldsymbol{u} = [u_1, u_2, \cdots, u_6]^T$ represents the vector of control signals, $\boldsymbol{q} = [\theta_1, \theta_2]^T$ indicates the joint angles, $\boldsymbol{f} = [f_1, f_2, \cdots, f_6]^T$ refers to the muscle forces, $\boldsymbol{\tau} = [\tau_1, \tau_2]^T$ denotes the joint torques that are related to the muscle forces, the matrix of time constants $\boldsymbol{T}$ is diag$[T_1, T_2, \cdots, T_6]$, and $\boldsymbol{f}_c = [f_{c1}, f_{c2}, \cdots, f_{c6}]^T$ represents the intrinsic muscle forces.

$$\boldsymbol{M}(\boldsymbol{q}) = \begin{bmatrix} I_1 + I_2 + 2M_2L_1S_2\cos\theta_2 + M_2L_1^2 & I_2 + M_2L_1S_2\cos\theta_2 \\ I_2 + M_2L_1S_2\cos\theta_2 & I_2 \end{bmatrix}, \tag{2}$$

$$\boldsymbol{C}(\boldsymbol{q},\dot{\boldsymbol{q}}) = \begin{bmatrix} -M_2L_1S_2(2\dot{\theta}_1+\dot{\theta}_2)\dot{\theta}_2\sin\theta_2 \\ M_2L_1S_2\dot{\theta}_1{}^2\sin\theta_2 \end{bmatrix}. \tag{3}$$

Table 1: Parameters of the two-link arm model

Parameter	Link 1	Link 2
M_i [kg]	1.59	1.44
L_i [m]	0.30	0.35
I_i [kgm^2]	0.18	0.21
S_i [cm]	6.78	7.99

The parameters of the two-link arm model are given in Table 1 [8]. The dynamics of the muscle forces have the low-pass filter property in that the muscle force changes smoothly [9], and the time constant T_i is set as 0.2 s.

The intrinsic muscle forces $\boldsymbol{f}_c$ are determined as follows:

$$\boldsymbol{f}_c(\boldsymbol{u}) = \boldsymbol{u} + \boldsymbol{D}\dot{\boldsymbol{l}} + \boldsymbol{K}(\boldsymbol{l} - \boldsymbol{l}_e) \tag{4}$$

where $\boldsymbol{l} = [l_1, l_2, \cdots, l_6]^T$ denotes the vector of muscle lengths, $\boldsymbol{l}_e$ represents the vector of muscle natural lengths, the matrix of viscosity coefficients $\boldsymbol{D}$ is diag$[d_1, d_2, \cdots, d_6]$, and the matrix of the elasticity coefficients $\boldsymbol{K}$ is diag$[k_1, k_2, \cdots, k_6]$. The coefficients k_i and d_i are set as 1.0×10^3 N/m and 2.5×10^3 Ns/m, respectively. The muscle length vector $\boldsymbol{l}$ is described as

$$\boldsymbol{l} = \boldsymbol{G}\boldsymbol{q} + \boldsymbol{l}_0 \tag{5}$$

$$\boldsymbol{G} = \begin{bmatrix} -a_1 & a_1 & 0 & 0 & -a_3 & a_3 \\ 0 & 0 & -a_2 & a_2 & -a_4 & a_4 \end{bmatrix}^T \tag{6}$$

where $\boldsymbol{G}$ represents the matrix of the moment arms, a_i denotes the moment arm (Table 2), and $\boldsymbol{l}_0$ indicates the muscle length for $\boldsymbol{q} = \boldsymbol{0}$. Then, the following equation is derived from Eqs. (4) and (5):

$$\boldsymbol{f}_c(\boldsymbol{u}) = \boldsymbol{u} + \boldsymbol{D}\boldsymbol{G}\dot{\boldsymbol{q}} + \boldsymbol{K}\boldsymbol{G}(\boldsymbol{q} - \boldsymbol{q}_e) \tag{7}$$

where $\boldsymbol{q}_e$ denotes the non-singular angle for the natural length $\boldsymbol{l}_e$. The non-singular angle $\boldsymbol{q}_e$ is assumed to be the joint angle for the target position $\boldsymbol{p}_e$. On the other hand, the joint torque $\boldsymbol{\tau}$ is described as

$$\boldsymbol{\tau} = -\boldsymbol{G}^T\boldsymbol{f}. \tag{8}$$

Then, the alternative dynamics of the musculoskeletal system are derived by substituting Eqs. (4) and (8) into Eq. (1).

$$\frac{d}{dt}\begin{bmatrix} \boldsymbol{q} \\ \dot{\boldsymbol{q}} \\ \boldsymbol{f} \end{bmatrix} = \boldsymbol{g}(\boldsymbol{x}, \boldsymbol{u}) = \begin{bmatrix} \dot{\boldsymbol{q}} \\ \boldsymbol{M}^{-1}(\boldsymbol{q})(-\boldsymbol{C}(\boldsymbol{q}, \dot{\boldsymbol{q}}) - \boldsymbol{G}^T\boldsymbol{f}) \\ \boldsymbol{T}^{-1}\{-\boldsymbol{f} + \boldsymbol{u} + \boldsymbol{D}\boldsymbol{G}\dot{\boldsymbol{q}} + \boldsymbol{K}\boldsymbol{G}(\boldsymbol{q} - \boldsymbol{q}_e)\} \end{bmatrix} \tag{9}$$

2.3 LQR controller

We obtained the control signals by using an LQR [7]. The linearized model of the musculoskeletal system around a non-singular point $(\boldsymbol{x}^*, \boldsymbol{u}^*)$ is described as

$$\frac{d}{dt}\bar{\boldsymbol{x}} = \boldsymbol{A}\bar{\boldsymbol{x}} + \boldsymbol{B}\bar{\boldsymbol{u}} \tag{10}$$

Table 2: Moment arms of muscles.

Parameter	a_1	a_2	a_3	a_4
Moment arm [cm]	4.0	2.5	3.5	3.0

where $\bar{\boldsymbol{x}} = \boldsymbol{x} - \boldsymbol{x}^*$, $\bar{\boldsymbol{u}} = \boldsymbol{u} - \boldsymbol{u}^*$,

$$\boldsymbol{A} = \frac{\partial \boldsymbol{g}}{\partial \boldsymbol{x}}(\boldsymbol{x}^*, \boldsymbol{u}^*), \qquad \boldsymbol{B} = \frac{\partial \boldsymbol{g}}{\partial \boldsymbol{u}}(\boldsymbol{x}^*, \boldsymbol{u}^*) \tag{11}$$

The non-singular point is set as $([\boldsymbol{q}_e, \boldsymbol{0}_{1\times 8}]^T, \boldsymbol{0})$. The evaluation function J is

$$J = \bar{\boldsymbol{x}}^T(t_f)\boldsymbol{Q}_f\bar{\boldsymbol{x}}(t_f) + \int_0^{t_f} (\bar{\boldsymbol{x}}^T\boldsymbol{Q}\bar{\boldsymbol{x}} + \bar{\boldsymbol{u}}^T\boldsymbol{R}\bar{\boldsymbol{u}})dt \tag{12}$$

where t_f denotes the movement duration, $\boldsymbol{Q}_f = \mathrm{diag}(2\alpha\times 10^7, 2\alpha\times 10^7, 5\times 10^6, 5\times 10^6, 10, 10, 10, 10, 10, 10)$, $\boldsymbol{Q} = \boldsymbol{0}$, and $\boldsymbol{R} = \beta\times\mathrm{diag}(1, 1, 1, 1, 1, 1)$. α is set as 0.1, 0.25, and 1.0, and β is set as 1.0, 5.0, and 10.0. Then, the optimal control signal $\boldsymbol{u}$ takes the following form:

$$\boldsymbol{u} = -\boldsymbol{R}^{-1}\boldsymbol{B}^T\boldsymbol{P}(t)\bar{\boldsymbol{x}}. \tag{13}$$

The matrix $\boldsymbol{P}$(t) is obtained from the following Ricatti differential equation running backward in time from $t = t_f$:

$$\dot{\boldsymbol{P}}(t) = -\boldsymbol{A}^T\boldsymbol{P}(t) - \boldsymbol{P}(t)\boldsymbol{A} + \boldsymbol{P}(t)\boldsymbol{B}\boldsymbol{R}^{-1}\boldsymbol{B}^T\boldsymbol{P}(t) - \boldsymbol{Q}, \tag{14}$$

$$\boldsymbol{P}(t_f) = \boldsymbol{Q}_f. \tag{15}$$

2.4 Positional variance

The signal-dependent noise $\boldsymbol{w}$(t) was added to the optimal control signal $\boldsymbol{u}$(t). The applied noise was the Gaussian noise, in which the mean was zero and the variance was $\gamma|u_i|^2$, where γ was set as 1.0.

The positional variance of the hand in the horizontal plane was estimated using a Monte Carlo simulation with 1000 repetitions. The variance σ_{xy}^2 was defined as the sum of the variance σ_x^2 and the variance σ_y^2 in accordance with [3].

The state vector of the musculoskeletal system and the matrix $\boldsymbol{P}$ of the Ricatti differential equation were updated by using the fourth-order Runge-Kutta method. The initial values of the state vector $\boldsymbol{x}(0)$ were set as $[\boldsymbol{q}(0), \dot{\boldsymbol{q}}(0), \boldsymbol{f}(0)]^T$, where the inverse kinematics was used for determining the initial angles $\boldsymbol{q}(0)$ for the start position $\boldsymbol{p}_s$, $\dot{\boldsymbol{q}}(0)$=[0, 0]^T, and $\boldsymbol{f}(0) = [0, 0, 0, 0, 0, 0]^T$. The time step was set as 1 ms.

3 Result

Figure 2 (a) shows the optimal trajectory of the hand position based on the LQR. The optimal trajectory of the hand position exhibits an almost straight line. Figure 2 (b) shows the hand speed profile. The speed profile exhibits a

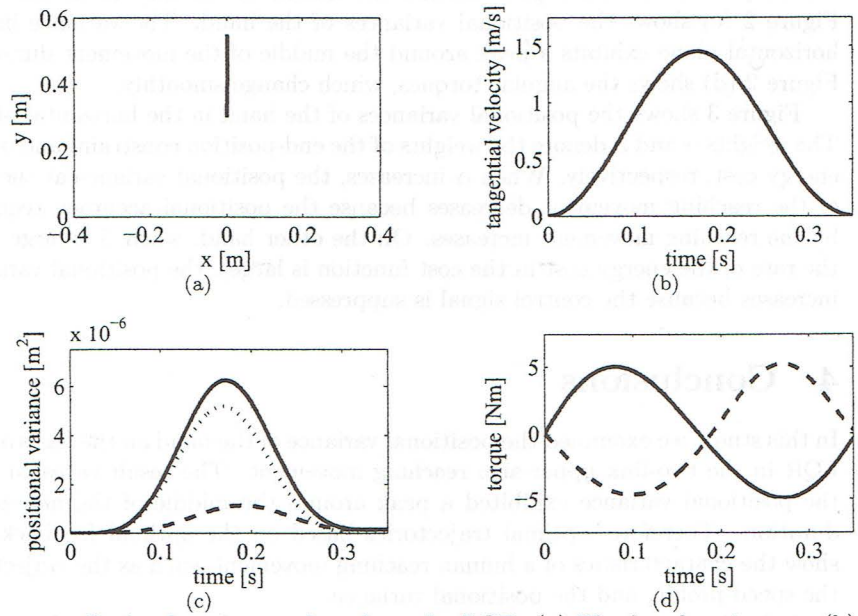

Figure 2: Optimal trajectory based on the LQR. (a) The hand trajectory, (b) the hand speed profile, (c) the positional variances of the hand (The solid line, the dashed line, and the dotted line show the variances in the horizontal plane, the x direction, and the y direction, respectively), (d) the angular torques (The solid line and the dashed line show the torques of the shoulder and of the elbow, respectively).

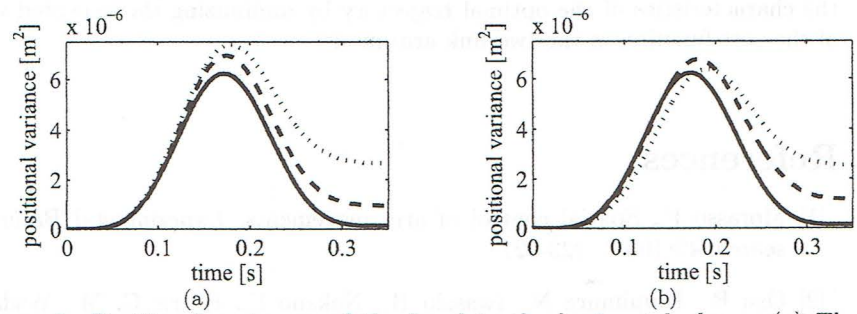

Figure 3: Positional variances of the hand in the horizontal plane. (a) The variances for $\alpha = 0.1$, 0.25, 1.0 and $\beta = 1.0$ are represented by a dotted line, a dashed line, and a solid line, respectively. (b) The variances for $\alpha = 1.0$ and $\beta = 1.0$, 5.0, 10.0 are represented by a solid line, a dashed line, and a dotted line, respectively.

bell-shaped curve with a peak around the middle of the movement duration. Figure 2 (c) shows the positional variances of the hand. The variance in the horizontal plane exhibits a peak around the middle of the movement duration. Figure 2 (d) shows the angular torques, which change smoothly.

Figure 3 shows the positional variances of the hand in the horizontal plane. The weights α and β denote the weights of the end-position constraint and of the energy cost, respectively. When α increases, the positional variance at the end of the reaching movement decreases because the positional accuracy required by the reaching movement increases. On the other hand, when β is large (i.e., the rate of the energy cost in the cost function is large), the positional variance increases because the control signal is suppressed.

4 Conclusions

In this study, we examined the positional variance of the hand on the basis of the LQR in the two-link upper-arm reaching movement. The result revealed that the positional variance exhibited a peak around the middle of the movement duration. Therefore, optimal trajectories based on the optimal feedback can show the characteristics of a human reaching movement, such as the trajectory, the speed profile, and the positional variance.

It has been reported that the positional variance of the hand decreases with a decrease in the target size in a one-link reaching movement of a human [2]. We examined the positional variances for the weights of the cost function. The result revealed that the optimal trajectory based on the LQR can represent the positional variance for the target size. The central nervous system might select the weights for the target size.

We adapted the LQR for the nonlinear two-link musculoskeletal system, and the optimal control signal was corrupted by the signal-dependent noise. Although the iLQG was used in the previous studies [4][5], we used the LQR to easily examine the characteristics of the LQR and could represent the characteristics of the human reaching movement. In the future, we might have to examine the characteristics of the optimal trajectory by minimizing the expected value of the cost function in the two-link arm model.

References

[1] Morasso P., Spatial control of arm movements, *Experimental Brain Research*, 42(1981), 223-227.

[2] Osu R., Kamimura N., Iwasaki H., Nakano E., Harris C. M., Wada Y. and Kawato M., Optimal impedance control for task achievement in the presence of signal-dependent noise, *Journal of Neurophysiology*, 92(2004), 1199-1215.

[3] Morishige K., Osu R., Miyamoto H. and Kawato M., The sources of variability in the time course of reaching movements, in Brain-Inspired IT II, International Congress Series 1291, edited by Ishii K., Natsume K., Hanazawa A., *Elsevier*, 105-108, 2006.

[4] Liu D. and Todorov E., Evidence for the flexible sensorimotor strategies predicted by optimal feedback control, *Journal of Neuroscience*, 27(2007), 9354-9368.

[5] Todorov E. and Li W., A generalized iterative LQG method for locally-optimal feedback control of constrained nonlinear stochastic systems, *Proceedings of American Control Conference*, 1(2005), 300-306.

[6] Rigoux L. and Guigon E., A model of reward- and effort-based optimal decision making and motor control, *PLoS Computational Biology*, 8(2012), e1002716.

[7] Tomi N., Gouko M. and Ito K., Combined mechanisms of internal model control and impedance control under force fields, in Artificial Neural Networks - ICANN2009, Lecture Notes in Computer Science 5768, edited by Alippi C., Polycarpou M., Panayiotou C., and Ellinas G., *Springer Berlin Heidelberg*, 628-637, 2009.

[8] Kambara H., Kim K., Shin D., Sato M. and Koike Y., Learning and generation of goal-directed arm reaching from scratch, *Neural Networks*, 22(2009), 348-361.

[9] Mannard A. and Stein R. B., Determination of the frequency response of isometric solues muscle in the cat using random nerve stimulation, *Journal of Physiology*, 229(1973), 275-296.